INORGANIC CHEMISTRY FRONTIERS

RESEARCH ARTICLE

View Article Online
View Journal | View Issue

Check for updates

Cite this: *Inorg. Chem. Front.*, 2024, **11**, 8431

Water-stable zero-dimensional hybrid zinc halide modulated by π–π interactions: efficient blue light emission and third-order nonlinear optical response†

Jia-Wei Li,*[a] Wenke Dong,[a] Yanjie Liu,[a] Yuhan Li,[a] Lu-Yuan Qiao,[a] Guang-Lu Liu,[a] Hui Zhang,[a] Chunjie Wang,[a] Hui-Li Zheng*[b] and Jian-Qiang Zhao *[b]

Achieving multifunctional optimization of halide optical materials through the precise modulation of intermolecular interactions is highly significant, yet it faces considerable challenges. Here, we propose a strategy of π–π interactions microregulating to achieve the simultaneous optimization of multiple properties of halide optical materials. Using this strategy, we obtained a new lead-free zero-dimensional (0D) zinc halide [DPE]$ZnCl_4$ (DPE = 1,2-di(4-pyridyl)ethylene), in which the protonated DPE cations are orderly arranged *via* π–π interactions, facilitating the ordered embedding and local regulation of $[ZnCl_4]^{2-}$ units within long-range one-dimensional cationic π–π stacking. As a result of these modifications, [DPE]$ZnCl_4$ exhibits efficient blue light emission with a high photoluminescent quantum yield (PLQY) of 18.55%, far exceeding that of corresponding organic salt halides. Furthermore, this compound demonstrates an enhanced third-order nonlinear optical (NLO) response, with the modulation depth and the third-order NLO absorption coefficient reaching 0.70 and 3.81 × 10^{-10} m W^{-1}, respectively, surpassing those of three-dimensional (3D) perovskite quantum dots and most organic–inorganic hybrid halides. Notably, the modulation of π–π interactions results in a significant breakthrough in water resistance, allowing [DPE]$ZnCl_4$ to maintain excellent structural and performance stability in water for a week. This innovative strategy of π–π interaction modulation provides new avenues for the multifunctional regulation and waterproof design of halide optical materials, and it is expected to advance the development and functionalization of stable halide optical materials.

Received 28th August 2024,
Accepted 21st October 2024

DOI: 10.1039/d4qi02194k

rsc.li/frontiers-inorganic

Published on 22 oktober 2024. Downloaded on 12.12.2025 10:24:23.

Introduction

Three-dimensional (3D) lead halide perovskite quantum dots (PQDs) have several advantages, including a high light absorption coefficient, excellent photoelectric activity, efficient carrier transport and tunable emission wavelengths, making them promising for applications in light-emitting diodes (LEDs), solar cells, photodetectors, and X-ray scintillators.[1–5] However, their low stability, high environmental sensitivity, lead toxicity, and aggregation-induced emission quenching present significant challenges for optical applications.[6–8] In this context, low-dimensional hybrid metal halides derived from 3D PQDs, featuring diverse structures and tunable emission properties, have emerged.[9–11] Particularly for zero-dimensional (0D) hybrid metal halides, spatially isolated inorganic structural units are usually encapsulated by insulating organic matrices, forming a strong quantum confinement effect that promotes high carrier localization and enhances emission efficiency.[12–16] By carefully selecting organic cations and metal halides, and controlling synthesis conditions, it is possible to achieve periodic embedding of halide units within organic cation assemblies, allowing for diverse structural and functional regulation. Consequently, combining environmentally friendly metal ions such as Sb^{3+}, In^{3+}, Mn^{2+}, and Zn^{2+} with various types and functionalities of organic cations endows hybrid metal halides with enhanced prospects and significant future potential.[17–21]

To date, a variety of strategies have been developed to effectively regulate the structure and photoluminescence (PL) properties of 0D hybrid metal halides, including adjusting the

[a]*School of Chemistry and Chemical Engineering, Zhoukou Normal University, Zhoukou, 466001, China. E-mail: lijw1990@zknu.edu.cn*
[b]*State Key Laboratory of Structural Chemistry Fujian Institute of Research on the Structure of Matter, Chinese Academy of Sciences, Fuzhou, 350002, China. E-mail: zhenghuili@fjirsm.ac.cn, jqzhao_15@163.com*

†Electronic supplementary information (ESI) available: All the experimental details, crystallographic data collection and refinement statistics, the details of the chemical synthesis, and supporting figures and tables. CCDC 2355212 for [DPE]$ZnCl_4$. For ESI and crystallographic data in CIF or other electronic format see DOI: https://doi.org/10.1039/d4qi02194k

Published on 22 oktober 2024. Downloaded on 12.12.2025 10:24:23.

coordination configuration of metals, increasing distortion within the coordination configuration, optimizing the aggregation state of halide units, and expanding the distance between isolated units.[22–26] Numerous 0D lead-free metal hybrid halides with outstanding performance have been reported and widely applied in LEDs, X-ray scintillation, anti-counterfeiting, and information encryption–decryption.[27–30] However, the design and performance optimization of most halides are primarily achieved through the modification and regulation of anionic groups. In contrast, the synthesis and functional regulation of 0D halides guided from the perspective of organic cations remain relatively rare. Significantly, as an indispensable component of hybrid metal halides, organic cations play a role beyond merely charge balance and the confinement and regulation of halide units.[31,32] Their intrinsic properties and potential functions warrant further exploration. In particular, designing and regulating the packing modes and intermolecular interactions between organic cations and metal halides is expected to further manipulate their photophysical properties and even introduce additional functional attributes, achieving multifunctionalization of new hybrid metal halide materials.[33–35] For instance, Lei *et al.* used $[BTPP]^+$ (BTPP = benzyltriphenylphosphonium) as an organic cation to obtain highly efficient dual-emission zinc-based halide phosphorescent materials through the heavy atom effect.[36] In this material, the $ZnBr_4^{2-}$ unit exhibits strong blue emission derived from self-trapping exciton (STE), while the $[BTPP]^+$ cation shows efficient green phosphorescence emission. This synergistic regulation of organic–inorganic components significantly activated the originally dormant phosphorescence properties of organic cation, resulting in highly efficient and long-lifetime room temperature afterglow, which utilized in time-color dual-resolved optical anti-counterfeiting and information encryption. Therefore, regulating the optical activity and functionality of metal halides through organic components and their spatial interactions is of great significance and presents considerable challenges.

Except for photophysical activity and functionalization, the extreme sensitivity and instability of hybrid metal halides to water and humid air further exacerbate their predicament.[37–40] This weak resistance to water and humidity not only diminishes the intrinsic activity and application potential of these materials but also poses serious environmental challenges due to the release of metal ions following hydrolysis, particularly Pb^{2+}.[33,41,42] Therefore, improving water stability is essential for advancing the development of perovskites and hybrid metal halides. Although the stability of PQDs has been significantly enhanced through porous material encapsulation strategies, the complexity of these processes and the risks of leakage after encapsulation have prompted researchers to seek more effective strategies.[43–48] Consequently, developing new methods to improve the inherent water stability of metal halides is urgently needed.

Inspired by the design concepts of metal–organic frameworks (MOFs) and hydrogen-bond organic frameworks (HOFs), introducing strong conjugated groups to form robust supramolecular structures connected by strong non-covalent interactions is expected to enhance the water resistance of the system.[49–51] These strong non-covalent interactions between conjugated groups offer greater stability than hydrogen bonds with water molecules, effectively preventing water erosion of the halide units protected by organic cations and thus avoiding metal ion hydrolysis. Additionally, these supramolecular structures connected by non-covalent interactions could also promote rapid charge transfer, leading to new functionalities inspired by ultrafast charge transport.[52] Thus, designing and screening specific organic cations and rationally manipulating their spatial interactions are expected to create highly stable and multifunctional halide optical materials, offering new prospects for the revival of metal halides.

Based on the above considerations, here we selected 1,2-di(4-pyridyl)ethylene (DPE) with bidirectional conjugated structures as the organic cation and template agent, and synthesized a hybrid lead-free metal halide $[DPE]ZnCl_4$ based on isolated $[ZnCl_4]^{2-}$ unit. As expected, the protonated DPE cations are arranged orderly through π–π interactions, forming a one-dimensional (1D) supramolecular stacking. This regulation of intermolecular non-covalent interactions not only significantly improves blue light emission efficiency but also imparts the material enhanced third-order nonlinear optical (NLO) activity, with the modulation depth and third-order NLO absorption coefficients surpassing those of 3D PQDs and most organic–inorganic hybrid halides. Most importantly, modulation of π–π interactions has led to a significant breakthrough in water resistance of halides maintaining excellent structural and performance stability after immersion in water for a week. This π–π interaction regulation strategy involving conjugated organic cations paves the new way for the precise design and long-term utilization of stable and multifunctional hybrid metal halide optical materials.

Results and discussion

Using DPE as the organic building block and $ZnCl_2$ as the metal source, colorless crystals of $[DPE]ZnCl_4$ were obtained through a self-assembly reaction under solvothermal conditions. X-ray single crystal diffraction analysis reveals that $[DPE]ZnCl_4$ crystallizes in the monoclinic space group $C2/c$, containing isolated $[ZnCl_4]^{2-}$ tetrahedral anions, protonated DPE cations and solvent water molecules (Fig. 1). In the $[ZnCl_4]^{2-}$ anion, each Zn^{2+} ion is coordinated with four Cl^-, forming a slightly distorted tetrahedral structure, with the Zn–Cl bond lengths ranging from 2.26 to 2.28 Å. Interestingly, the protonated $[DPE]^{2+}$ cations are arranged orderly through strong π–π interactions from pyridine rings with adjacent cations, with a distance of 3.67 Å between the central rings of adjacent cations. This arrangement results in long-range 1D cationic π–π stacking, which contribute to enhancing the structural stability for $[DPE]ZnCl_4$ and the interaction and energy transfer of localized electrons. All $[ZnCl_4]^{2-}$ polyhedra are periodically embedded into the DPE organic matrix, forming a

 This journal is © the Partner Organisations 2024

Published on 22 oktober 2024. Downloaded on 12.12.2025 10:24:23.

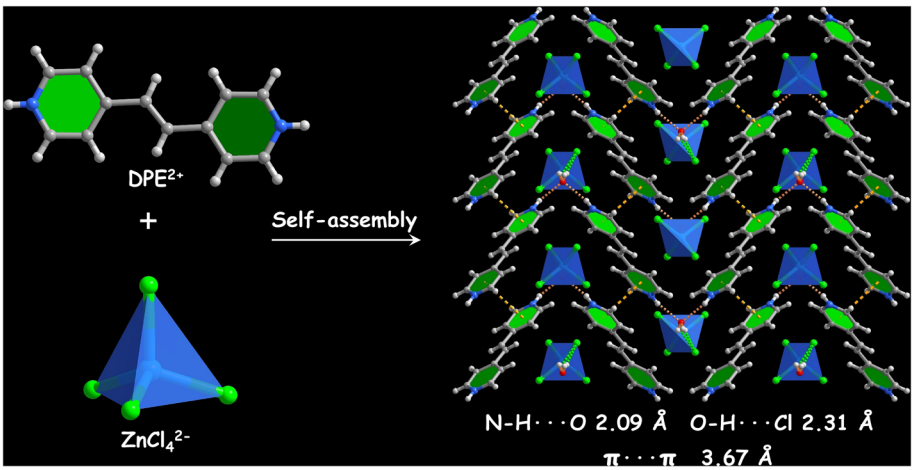

Fig. 1 Schematic diagram of structure assembly of [DPE]$ZnCl_4$. Color legends: cyan, Zn; green, Cl; blue, N; gray, C; red, O; white H.

perfect 0D hybrid structure. In this structure, the hydrogen on the pyridine N forms strong hydrogen bonds (N–H···O 2.09 Å) with free water molecules, while the hydrogen on the water molecules forms weak hydrogen bonds (O–H···Cl 2.31 Å) with the Cl^- from $[ZnCl_4]^{2-}$. These multiple hydrogen bonds and strong π–π interactions ensure the firm integration of the organic cation $[DPE]^{2+}$ and the inorganic anion $[ZnCl_4]^{2-}$ within the hybrid structure. The experimental powder X-ray diffraction (PXRD) patterns of [DPE]$ZnCl_4$ matched well with the simulated based on single-crystal structural, indicating a phase-pure sample (Fig. S1†). The thermal stability of [DPE]$ZnCl_4$ was characterized by thermal analysis, and the results show that the compound can remain stable up to 220 °C (Fig. S2†). The morphology of [DPE]$ZnCl_4$ was characterized using field emission scanning electron microscopy (FE-SEM), revealing a ribbon-like structure with a length exceeding 100 μm (Fig. S3†). Energy dispersive spectroscopy (EDS) and elemental mapping images indicated that Zn, Cl, C, and N are uniformly distributed throughout the crystal (Fig. S4†).

The optical properties of [DPE]$ZnCl_4$ were characterized by solid-state UV-Visible absorption, steady-state, and time-resolved PL emission spectroscopy. The UV-Vis absorption spectrum indicates a strong absorption peak around 305 nm with the cutoff wavelength at 376 nm (Fig. S5a†). The band gap of [DPE]$ZnCl_4$ was estimated to be 3.27 eV according to the Tauc formula, which corresponds to the colorless appearance (Fig. S5b†). As shown in Fig. 2a, under the irradiation of 365 nm ultraviolet light, the colorless needle-shaped crystals of [DPE]$ZnCl_4$ emit a strong blue light. The compound exhibits a broad excitation spectrum in the 200–400 nm range, accompanied by two excitation peaks at 282 nm and 370 nm. Under ultraviolet excitation at 370 nm, [DPE]$ZnCl_4$ exhibits a narrowband blue emission with a maximum emission peak at 429 nm (Fig. 2b). The full width at half maximum (FWHM) and the Stokes shift were measured to be 29 and 59 nm, respectively, which are smaller than that of reported hybrid zinc halides, such as (EP)$ZnBr_4$ (79 nm), (TMPDA)$ZnBr_4$ (78 nm), [H_2MPz]$ZnBr_4$ (86 nm).[53] The narrowband emission has the Commission Internationale de l'Eclairage (CIE) chromaticity coordinates of (0.174, 0.072), corresponding to the observed blue emission (Fig. 2c). Under the ultraviolet light excitation at 370 nm, the PLQY of [DPE]$ZnCl_4$ was measured as 18.55%, significantly exceeding that of the inorganic hybrid Cs_2ZnBr_4 (< 5%) and many other reported blue-light emitting perovskite halides (Fig. S6†).[54–56] To elucidate the dynamics of its radiative transitions, time-resolved PL spectra were measured at room temperature with the maximum emission wavelength of 429 nm. As shown in Fig. 2d, the PL decay curve can be fitted with a single exponential function to give a short lifetime of 8.12 ns, which indicates a single radiation path. Considering its broad excitation spectrum, we further conducted emission spectra related to excitation wavelengths at 300 K. Under ultraviolet excitation in the range of 230–400 nm, [DPE]$ZnCl_4$ exhibits the same narrowband emission profile and only one dominant emission center in the 3D excitation and emission correlation map, indicating a single radiative PL mechanism (Fig. 2e and Fig. S7†). To further understand the PL mechanism, we analyzed the PL spectrum of organic cation salts of [DPE]Cl_2, which exhibited a similar emission spectrum to [DPE]$ZnCl_4$ with the maximum emission peak at 405 nm upon exciting with 329 nm light (Fig. S8†). The similar emission spectrum shape and emission position indicate that the PL of [DPE]$ZnCl_4$ originates from organic salts. Moreover, the time-resolved PL spectrum of the organic salt can be fitted by a single exponential function with a lifetime of 2.66 ns, comparable to that of [DPE]$ZnCl_4$, further elucidates that the emission of [DPE]$ZnCl_4$ is attributed to the organic salt [DPE]Cl (Fig. S9†). It is worth noting that compared with the high PLQY of [DPE]$ZnCl_4$, the organic salt emitted almost no light under ultraviolet light, accompanied by negligible PLQY. This indicates that the filling of halide anions and the ordered π–π interaction of molecules effectively suppress the fluorescence quenching effect and the probability

Published on 22 oktober 2024. Downloaded on 12.12.2025 10:24:23.

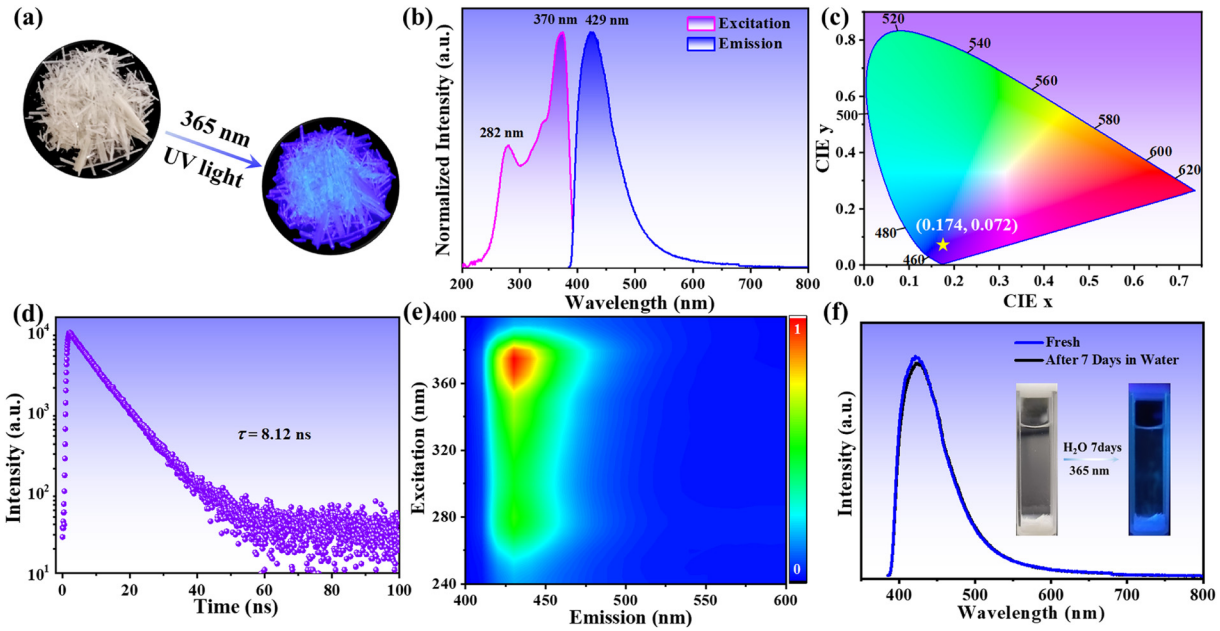

Fig. 2 Photoluminescence characterizations of $[DPE]ZnCl_4$. (a) Photos of crystals in sunlight and ultraviolet light of 365 nm; (b) excitation and emission spectra; (c) the CIE coordinates; (d) the PL decay curve at 429 nm at 300K; (e)the 3D excitation and emission correlation map; (f) comparison of the PL spectrum before and after immersion in water for 7 days.

of non-radiative transition, thereby significantly enhancing its PL efficiency.

Due to the strong π–π interactions between molecules, we further investigated the water stability of $[DPE]ZnCl_4$ by immersing the crystals in distilled water for a week. The results demonstrated that after one week of immersion, the crystals maintained both their shape and transparency, while continuing to emit bright blue light under ultraviolet light (Fig. 2f). The PL spectra of freshly prepared samples and those immersed in water for one week remained consistent, with no significant decrease observed, thereby indicating remarkable stability. Similarly, PXRD spectrum of samples after one week of immersion showed that all peaks matched well with those of the fresh samples, confirming their structural stability (Fig. S10†). In addition, the morphology of $[DPE]ZnCl_4$ showed no significant change before and after immersion in water for 7 days (Fig. S11). To determine whether the samples dissolved in water, we evaporated the separated water and found no obvious precipitate after complete evaporation. Additionally, inductively coupled plasma mass spectrometry (ICP-MS) testing of the solution after immersion showed a Zn^{2+} concentration of 3.2 mg L^{-1}, further indicating the negligible leaching of Zn ions from the material. These results demonstrate that by regulating the π–π interactions between organic cations, the water stability of the halide can be significantly enhanced, providing an effective solution for reducing environmental pollution and enabling its application under harsh conditions.

The strong π–π interactions in $[DPE]ZnCl_4$ prompted further investigation into its third-order NLO properties. We combined $[DPE]ZnCl_4$ with polydimethylsiloxane (PDMS) to prepare a flexible, transparent $[DPE]ZnCl_4$@PDMS film. Under sunlight, this composite film exhibits high transmittance, allowing clear recognition of patterns behind the film (Fig. 3a). Under ultraviolet light irradiation, the film displays uniform bright blue luminescence, indicating that $[DPE]ZnCl_4$ is uniformly distributed within the polymer matrix (Fig. 3b). Notably, this film demonstrates good flexibility, allowing continuous folding and stretching without altering its shape, making it suitable as a flexible PL and third-order NLO material. The third-order NLO properties were evaluated using a standard open-aperture Z-scan system with a 532 nm nanosecond laser and a pulse energy of 4 μJ. At a laser pulse energy of 90 μJ, the pure PDMS film did not exhibit any nonlinear optical response, thus ruling out the influence of the substrate. As shown in Fig. 3c, the organic salt $[DPE]Cl_2$ exhibited slight reverse saturable absorption with a minimum normalized transmittance of 0.95 at its focus (Z = 0), demonstrating a weak third-order NLO response. In comparison, $[DPE]ZnCl_4$ exhibited an enhanced third-order nonlinear response with the modulation depth of up to 0.70, indicating excellent optical limiting properties. Further quantitative assessment of their third-order NLO responses, obtained by fitting the Z-scan curves, yielded a third-order nonlinear coefficient (β) for $[DPE]ZnCl_4$ of 3.81 × 10^{-10} m W^{-1}, which is 7.3 times greater than that of the organic salt $[DPE]Cl_2$. Additionally, the optical limiting thresholds (F_{OL}, defined as the input fluence at which the transmittance is half of the linear transmittance) for $[DPE]Cl_2$ and $[DPE]ZnCl_4$ were calculated to be 3.45 and 2.23 J cm^{-2}, respectively (Fig. 3d). These results indicate that by employing the π–π interactions microregulation strategy, we achieved a significant enhancement in the third-order nonlinear coefficient and modulation depth of $[DPE]ZnCl_4$, surpassing those

 This journal is © the Partner Organisations 2024

Published on 22 oktober 2024. Downloaded on 12.12.2025 10:24:23.

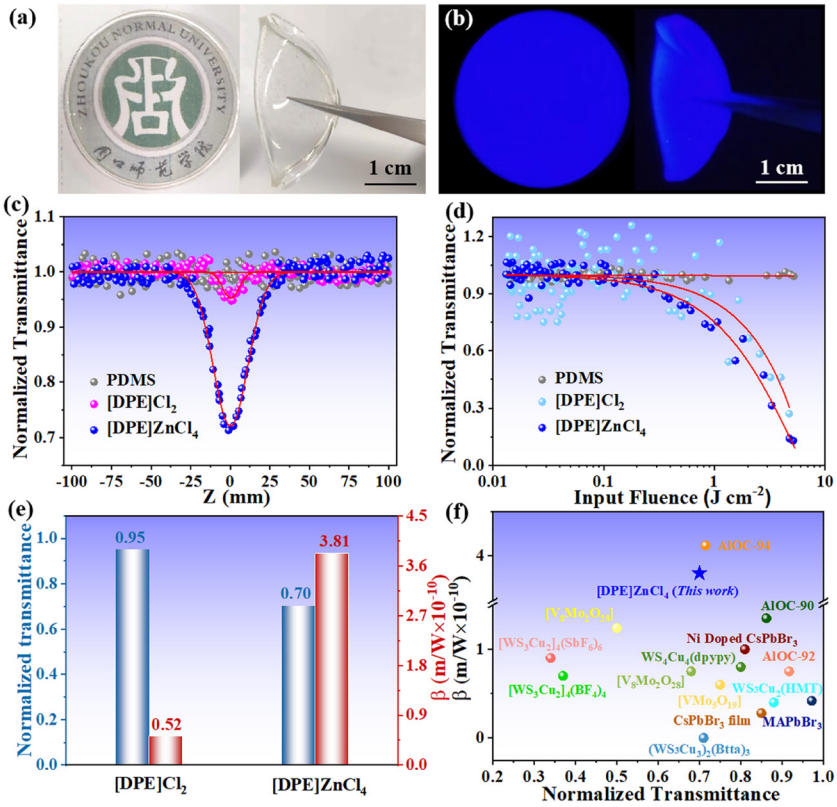

Fig. 3 (a and b) Photos of $[DPE]ZnCl_4$@PDMS films in sunlight and ultraviolet light of 365 nm; (c) the open-aperture Z-scan diagrams of $[DPE]Cl_2$ and $[DPE]ZnCl_4$ at 532 nm; (d) the curves of normalized transmittance *versus* input fluence; (e and f) comparison of the minimum normalized transmittance and the nonlinear absorption coefficients for $[DPE]Cl_2$, $[DPE]ZnCl_4$ and some representative crystalline materials reported.

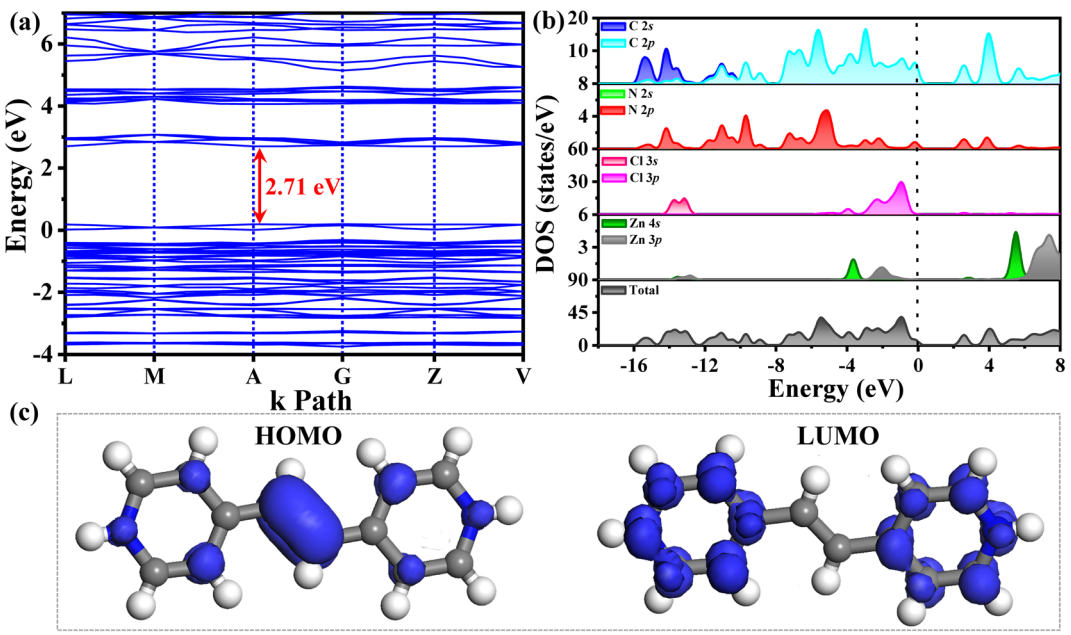

Fig. 4 Band structures and density of states of $[DPE]ZnCl_4$ (a and b); The frontier molecular orbits (HOMO and LUMO) of $[DPE]ZnCl_4$ (c).

Published on 22 oktoober 2024. Downloaded on 12.12.2025 10:24:23.

of the original organic salts, most PQDs materials, and other crystalline materials (Fig. 3e, f and Table S1†). Further precise structural analysis indicates that compared to the π–π interactions ($d_{Cg–Cg}$ = 4.75 Å) in the organic salt of [DPE]Cl, the incorporation and reassembly of the $[ZnCl]_4^{2-}$ structural unit significantly enhance the π–π interactions ($d_{Cg–Cg}$ = 3.67 Å) among the organic cations in $[DPE]ZnCl_4$ (Fig. S12†). This enhancement of intermolecular interactions leads to a significant improvement in the modulation depth and the NLO coefficients. This simple and effective microregulation strategy provides a new approach for developing high-performance hybrid metal halide third-order NLO materials.

Theoretical calculations based on density functional theory (DFT) were conducted to analyze the electronic structure and band gap of $[DPE]ZnCl_4$. As shown in Fig. 4a, the band structure calculations indicate that $[DPE]ZnCl_4$ has a direct band gap of 2.71 eV, consistent with the experimental band gap obtained from solid-state UV-Vis measurements. Furthermore, density of states (DOS) analysis shows that the conduction band minimum (CBM) and the valence band maximum (VBM) are primarily derived from the C-2p and N-2p states in the DPE cation, indicating that the organic cations significantly contribute to the band structure and electronic properties of $[DPE]ZnCl_4$ (Fig. 4b). This further supports the conclusion that PL originates from the organic cations. Orbital distribution analysis confirms that the lowest unoccupied molecular orbital (LUMO) is primarily located on the C=C bonds of the organic cation, while the highest occupied molecular orbital (HOMO) is chiefly situated on the pyridine ring, facilitating rapid ligand-to-ligand charge transfer (LLCT) (Fig. 4c). Consequently, strong intermolecular π–π interactions link organic cations to form non-covalently linked molecular wires, further enhancing efficient charge transfer within the lattice and boosting the third-order NLO properties.

Conclusions

In summary, we have developed a microregulation strategy involving π–π interactions to construct highly water-resistant multifunctional zinc halide optical materials. As a typical example guided by this strategy, $[DPE]ZnCl_4$ exhibits an ordered one-dimensional cation stacking mode induced by π–π interactions, thereby enhancing the rigidity and stability of the structure, effectively facilitating the regulation and efficient transfer of localized charges. With the microregulation of the aforementioned π–π interactions, $[DPE]ZnCl_4$ demonstrates efficient blue light emission and enhanced third-order NLO activity, with its PLQY and NLO coefficient significantly surpassing those of 3D PQDs and most organic–inorganic hybrid halides. More importantly, this simple structural microregulation strategy enhances the water resistance of $[DPE]ZnCl_4$, which can be stable in water for more than 7 days. This work realizes synergistic regulation and simultaneous optimization of multiple optical functions and stability in metal halides, providing new insights into the design and application of novel multifunctional metal halide perovskite materials with high stability, potentially expanding their applications across a broad chemical range and under extreme conditions.

Data availability

The data that support the findings of this study are available from the corresponding author upon reasonable request.

Conflicts of interest

There are no conflicts to declare.

Acknowledgements

This research was supported by the National Natural Science Foundation of China (22301317), Key Scientific and Technological Project of Henan Province (232102310376, 232102311181 and 242102110035), the Specialized Research Fund for the Doctoral Program of Zhoukou Normal University (ZKNUC2021021) and the University Student Scientific Research Innovation Foundation of Zhoukou Normal University (ZKNUD2024085).

References

1 J. Shamsi, A. S. Urban, M. Imran, L. De Trizio and L. Manna, Metal Halide Perovskite Nanocrystals: Synthesis, Post-Synthesis Modifications, and Their Optical Properties, *Chem. Rev.*, 2019, **119**, 3296–3348.
2 J. Luo, X. Wang, S. Li, J. Liu, Y. Guo, G. Niu, L. Yao, Y. Fu, L. Gao, Q. Dong, C. Zhao, M. Leng, F. Ma, W. Liang, L. Wang, S. Jin, J. Han, L. Zhang, J. Etheridge, J. Wang, Y. Yan, E. H. Sargent and J. Tang, Efficient and stable emission of warm-white light from lead-free halide double perovskites, *Nature*, 2018, **563**, 541–545.
3 Q. He, M. Worku, H. Liu, E. Lochner, A. J. Robb, S. Lteif, J. S. R. V. Winfred, K. Hanson, J. B. Schlenoff, B. J. Kim and B. Ma, Highly Efficient and Stable Perovskite Solar Cells Enabled by Low-Cost Industrial Organic Pigment Coating, *Angew. Chem., Int. Ed.*, 2021, **60**, 2485–2492.
4 Y. Zhou, J. Chen, O. M. Bakr and O. F. Mohammed, Metal Halide Perovskites for X-ray Imaging Scintillators and Detectors, *ACS Energy Lett.*, 2021, **6**, 739–768.
5 F. Zhou, Z. Li, W. Lan, Q. Wang, L. Ding and Z. Jin, Halide Perovskite: a Potential Scintillator for X-Ray Detection, *Small Methods*, 2020, **4**, 2000506.
6 J. Chen, H. Xiang, J. Wang, R. Wang, Y. Li, Q. Shan, X. Xu, Y. Dong, C. Wei and H. Zeng, Perovskite White Light Emitting Diodes: Progress, Challenges, and Opportunities, *ACS Nano*, 2021, **15**, 17150–17174.

 This journal is © the Partner Organisations 2024

Published on 22 oktober 2024. Downloaded on 12.12.2025 10:24:23.

7 L. N. Quan, F. P. García de Arquer, R. P. Sabatini and E. H. Sargent, Perovskites for Light Emission, *Adv. Mater.*, 2018, **30**, 1801996.
8 Y. Wei, Z. Cheng and J. Lin, An overview on enhancing the stability of lead halide perovskite quantum dots and their applications in phosphor-converted LEDs, *Chem. Soc. Rev.*, 2019, **48**, 310–350.
9 H. Lin, C. Zhou, Y. Tian, T. Siegrist and B. Ma, Low-Dimensional Organometal Halide Perovskites, *ACS Energy Lett.*, 2018, **3**, 54–62.
10 Y. Han, S. Yue and B.-B. Cui, Low-Dimensional Metal Halide Perovskite Crystal Materials: Structure Strategies and Luminescence Applications, *Adv. Sci.*, 2021, **8**, 2004805.
11 L.-J. Xu, S. Lee, X. Lin, L. Ledbetter, M. Worku, H. Lin, C. Zhou, H. Liu, A. Plaviak and B. Ma, Multicomponent Organic Metal Halide Hybrid with White Emissions, *Angew. Chem., Int. Ed.*, 2020, **59**, 14120–14123.
12 C. Zhou, L.-J. Xu, S. Lee, H. Lin and B. Ma, Recent Advances in Luminescent Zero-Dimensional Organic Metal Halide Hybrids, *Adv. Opt. Mater.*, 2021, **9**, 2001766.
13 R. Zhang, X. Mao, Y. Yang, S. Yang, W. Zhao, T. Wumaier, D. Wei, W. Deng and K. Han, Air-Stable, Lead-Free Zero-Dimensional Mixed Bismuth-Antimony Perovskite Single Crystals with Ultra-broadband Emission, *Angew. Chem., Int. Ed.*, 2019, **58**, 2725–2729.
14 L. Zhou, J.-F. Liao, Z.-G. Huang, X.-D. Wang, H.-Y. Chen and D.-B. Kuang, Intrinsic Self-Trapped Emission in 0D Lead-Free $(C_4H_{14}N_2)_2In_2Br_{10}$ Single Crystal, *Angew. Chem., Int. Ed.*, 2019, **58**, 15435–15440.
15 J.-Q. Zhao, M.-F. Han, X.-J. Zhao, Y.-Y. Ma, C.-Q. Jing, H.-M. Pan, D.-Y. Li, C.-Y. Yue and X.-W. Lei, Structural Dimensionality Modulation toward Enhanced Photoluminescence Efficiencies of Hybrid Lead-Free Antimony Halides, *Adv. Opt. Mater.*, 2021, **9**, 2100556.
16 Z.-B. Hu, X. Yang, J. Zhang, L.-A. Gui, Y.-F. Zhang, X.-D. Liu, Z.-H. Zhou, Y. Jiang, Y. Zhang, S. Dong and Y. Song, Molecular ferroelectric with low-magnetic-field magnetoelectricity at room temperature, *Nat. Commun.*, 2024, **15**, 4702.
17 Z. Xiao, Z. Song and Y. Yan, From Lead Halide Perovskites to Lead-Free Metal Halide Perovskites and Perovskite Derivatives, *Adv. Mater.*, 2019, **31**, 1803792.
18 Z. Wang, Z. Zhang, L. Tao, N. Shen, B. Hu, L. Gong, J. Li, X. Chen and X.-Y. Huang, Hybrid Chloroantimonates(III): Thermally Induced Triple-Mode Reversible Luminescent Switching and Laser-Printable Rewritable Luminescent Paper, *Angew. Chem., Int. Ed.*, 2019, **58**, 9974–9978.
19 D.-Y. Li, Y.-B. Shang, Q. Liu, H.-W. Zhang, X.-Y. Zhang, C.-Y. Yue and X.-W. Lei, 0D hybrid indium halide as a highly efficient X-ray scintillation and ultra-sensitive fluorescent probe, *Mater. Horiz.*, 2023, **10**, 5004–5015.
20 J.-B. Luo, J.-H. Wei, Z.-Z. Zhang, Z.-L. He and D.-B. Kuang, A Melt-Quenched Luminescent Glass of an Organic-Inorganic Manganese Halide as a Large-Area Scintillator for Radiation Detection, *Angew. Chem., Int. Ed.*, 2023, **62**, e202216504.
21 A. Yangui, R. Roccanova, T. M. McWhorter, Y. Wu, M.-H. Du and B. Saparov, Hybrid Organic–Inorganic Halides $(C_5H_7N_2)_2MBr_4$ (M = Hg, Zn) with High Color Rendering Index and High-Efficiency White-Light Emission, *Chem. Mater.*, 2019, **31**, 2983–2991.
22 R. Gao, M. S. Kodaimati and D. P. Yan, Recent advances in persistent luminescence based on molecular hybrid materials, *Chem. Soc. Rev.*, 2021, **50**, 5564–5589.
23 H.-L. Liu, H.-Y. Ru, M.-E. Sun, Z.-Y. Wang and S.-Q. Zang, Organic–Inorganic Manganese Bromide Hybrids with Water-Triggered Luminescence for Rewritable Paper, *Adv. Opt. Mater.*, 2021, **10**, 2101700.
24 D.-Y. Li, J.-H. Wu, X.-Y. Wang, X.-Y. Zhang, C.-Y. Yue and X.-W. Lei, Reversible Triple-Mode Photo- and Radioluminescence and Nonlinear Optical Switching in Highly Efficient 0D Hybrid Cuprous Halides, *Chem. Mater.*, 2023, **35**, 6598–6611.
25 J.-Q. Zhao, Y.-Y. Ma, X.-J. Zhao, Y.-J. Gao, Z.-Y. Xu, P.-C. Xiao, C.-Y. Yue and X.-W. Lei, Stepwise Crystalline Structural Transformation in 0D Hybrid Antimony Halides with Triplet Turn-on and Color-Adjustable Luminescence Switching, *Research*, 2023, **6**, 0094.
26 L. Mao, J. Chen, P. Vishnoi and A. K. Cheetham, The Renaissance of Functional Hybrid Transition-Metal Halides, *Acc. Mater. Res.*, 2022, **3**, 439–448.
27 J.-L. Li, Y.-F. Sang, L.-J. Xu, H.-Y. Lu, J.-Y. Wang and Z.-N. Chen, Highly Efficient Light-Emitting Diodes Based on an Organic Antimony(III) Halide Hybrid, *Angew. Chem., Int. Ed.*, 2021, **61**, e202113450.
28 H. Xiao, P. Dang, X. Yun, G. Li, Y. Wei, Y. Wei, X. Xiao, Y. Zhao, M. S. Molokeev, Z. Cheng and J. Lin, Solvatochromic Photoluminescent Effects in All-Inorganic Manganese(II)-Based Perovskites by Highly Selective Solvent-Induced Crystal-to-Crystal Phase Transformations, *Angew. Chem., Int. Ed.*, 2021, **60**, 3699–3707.
29 N. Lin, X. Wang, H.-Y. Zhang, K.-Q. Sun, L. Xiao, X.-Y. Zhang, C.-Y. Yue, L. Han, Z.-W. Chen and X.-W. Lei, Zero-Dimensional Copper(I) Halide Microcrystals as Highly Efficient Scintillators for Flexible X-ray Imaging, *ACS Appl. Mater. Interfaces*, 2024, **16**, 41165–41175.
30 J.-Q. Zhao, H.-S. Shi, L.-R. Zeng, H. Ge, Y.-H. Hou, X.-M. Wu, C.-Y. Yue and X.-W. Lei, Highly emissive zero-dimensional antimony halide for anti-counterfeiting and confidential information encryption-decryption, *Chem. Eng. J.*, 2022, **431**, 134336.
31 G. Xiao, X. Fang, Y.-J. Ma and D. Yan, Multi-Mode and Dynamic Persistent Luminescence from Metal Cytosine Halides through Balancing Excited-State Proton Transfer, *Adv. Sci.*, 2022, **9**, 2200992.
32 J.-H. Wei, W.-T. Ou, J.-B. Luo and D.-B. Kuang, Zero-Dimensional Zn-Based Halides with Ultra-Long Room-Temperature Phosphorescence for Time-Resolved Anti-Counterfeiting, *Angew. Chem., Int. Ed.*, 2022, **61**, e202207985.

Published on 22 oktoober 2024. Downloaded on 12.12.2025 10:24:23.

33 T. Sheikh, S. Maqbool, P. Mandal and A. Nag, Introducing Intermolecular Cation-π Interactions for Water-Stable Low Dimensional Hybrid Lead Halide Perovskites, *Angew. Chem., Int. Ed.*, 2021, **60**, 18265–18271.

34 F. Nie, K.-Z. Wang and D. Yan, Supramolecular glasses with color-tunable circularly polarized afterglow through evaporation-induced self-assembly of chiral metal–organic complexes, *Nat. Commun.*, 2023, **14**, 1654.

35 J. Li, J. Wu, Y. Xiao, L. Rao, R. Zeng, K. Xu, X.-C. Huang, J. Z. Zhang and B. Luo, Efficient triplet energy transfer in a 0D metal halide hybrid with long persistence room temperature phosphorescence for time-resolved anti-counterfeiting, *Inorg. Chem. Front.*, 2023, **10**, 7167–7175.

36 J.-Q. Zhao, D.-Y. Wang, T.-Y. Yan, Y.-F. Wu, Z.-L. Gong, Z.-W. Chen, C.-Y. Yue, D. Yan and X.-W. Lei, Synchronously Improved Multiple Afterglow and Phosphorescence Efficiencies in 0D Hybrid Zinc Halides with Ultrahigh Anti-Water Stabilities, *Angew. Chem., Int. Ed.*, 2024, **63**, e202412350.

37 J. Hou, P. Chen, A. Shukla, A. Krajnc, T. Wang, X. Li, R. Doasa, L. H. G. Tizei, B. Chan, D. N. Johnstone, R. Lin, T. U. Schülli, I. Martens, D. Appadoo, M. S. Ari, Z. Wang, T. Wei, S.-C. Lo, M. Lu, S. Li, E. B. Namdas, G. Mali, A. K. Cheetham, S. M. Collins, V. Chen, L. Wang and T. D. Bennett, Liquid-phase sintering of lead halide perovskites and metal-organic framework glasses, *Science*, 2021, **374**, 621–625.

38 C. Peng, X. Song, J. Yin, G. Zhang and H. Fei, Intrinsic White-Light-Emitting Metal–Organic Frameworks with Structurally Deformable Secondary Building Units, *Angew. Chem., Int. Ed.*, 2019, **58**, 7818–7822.

39 S. Seth, T. Ahmed, A. De and A. Samanta, Tackling the Defects, Stability, and Photoluminescence of $CsPbX_3$ Perovskite Nanocrystals, *ACS Energy Lett.*, 2019, **4**, 1610–1618.

40 C. Peng, Z. Zhuang, H. Yang, G. Zhang and H. Fei, Ultrastable, cationic three-dimensional lead bromide frameworks that intrinsically emit broadband white-light, *Chem. Sci.*, 2018, **9**, 1627–1633.

41 J. Hou, Z. Wang, P. Chen, V. Chen, A. K. Cheetham and L. Wang, Intermarriage of Halide Perovskites and Metal-Organic Framework Crystals, *Angew. Chem., Int. Ed.*, 2020, **59**, 19434–19449.

42 C. Zhang, B. Wang, W. Li, S. Huang, L. Kong, Z. Li and L. Li, Conversion of invisible metal-organic frameworks to luminescent perovskite nanocrystals for confidential information encryption and decryption, *Nat. Commun.*, 2017, **8**, 1138.

43 W. Liu, H. Fu, H. Liao, Z. Liang, Y. Ye, J. Zheng and W. Yang, In situ synthesis of coaxial $CsPbX_3$@polymer (X = Cl, Br, I) fibers with significantly enhanced water stability, *J. Mater. Chem. C*, 2020, **8**, 13972–13975.

44 P. Wang, B. Wang, Y. Liu, L. Li, H. Zhao, Y. Chen, J. Li, S. Liu and K. Zhao, Ultrastable perovskite-zeolite composite enabled by encapsulation and in situ passivation, *Angew. Chem., Int. Ed.*, 2020, **59**, 23100–23106.

45 H. Tsai, H.-H. Huang, J. Watt, C.-H. Hou, J. Strzalka, J.-J. Shyue, L. Wang and W. Nie, Cesium Lead Halide Perovskite Nanocrystals Assembled in Metal-Organic Frameworks for Stable Blue Light Emitting Diodes, *Adv. Sci.*, 2022, **9**, 2105850.

46 C. Zhang, Z.-S. Li, X.-Y. Dong, Y.-Y. Niu and S.-Q. Zang, Multiple Responsive CPL Switches in an Enantiomeric Pair of Perovskite Confined in Lanthanide MOFs, *Adv. Mater.*, 2022, **34**, 2109496.

47 Q. Zhang, W. Zheng, Q. Wan, M. Liu, X. Feng, L. Kong and L. Li, Confined Synthesis of Stable and Uniform $CsPbBr_3$ Nanocrystals with High Quantum Yield up to 90% by High Temperature Solid-State Reaction, *Adv. Opt. Mater.*, 2021, **9**, 2002130.

48 X.-W. Kong, L.-X. Wu, X. Yang, D.-Y. Wang, S.-X. Wang, S.-Y. Li, C.-Y. Yue, F. Yu and X.-W. Lei, Enhancing the Water-Stability of 1D Hybrid Manganese Halides by a Cationic Engineering Strategy, *Adv. Opt. Mater.*, 2024, **12**, 2302710.

49 H.-L. Zheng, J.-Q. Zhao, Y.-Y. Sun, A.-A. Zhang, Y.-J. Cheng, L. He, X. Bu, J. Zhang and Q. Lin, Multilevel-Regulated Metal–Organic Framework Platform Integrating Pore Space Partition and Open-Metal Sites for Enhanced CO_2 Photoreduction to CO with Nearly 100% Selectivity, *J. Am. Chem. Soc.*, 2023, **145**, 27728–27739.

50 W. Wei, L. He, G. Han, Y. Lu, S. Shi, Z. Yuan, X. Wang, Y. Li, B. Chen, Z. Zhang and S. Xiang, Stimulus-responsive hydrogen-bonded organic frameworks: Construction strategies, research progress and applications, *Coordin. Chem. Rev.*, 2024, **507**, 215760.

51 H. Li, C. Chen, Q. Li, X. J. Kong, Y. Liu, Z. Ji, S. Zou, M. Hong and M. Wu, An Ultra-stable Supramolecular Framework Based on Consecutive Side-by-side Hydrogen Bonds for One-step C_2H_4/C_2H_6 Separation, *Angew. Chem., Int. Ed.*, 2024, **63**, e202401754.

52 D.-J. Li, Q.-H. Li, Z.-R. Wang, Z.-Z. Ma, Z.-G. Gu and J. Zhang, Interpenetrated Metal-Porphyrinic Framework for Enhanced Nonlinear Optical Limiting, *J. Am. Chem. Soc.*, 2021, **143**, 17162–17169.

53 Y.-Y. Ma, Y.-M. Sun, W.-J. Xu, X.-L. Liu, Q.-Q. Zhong, Y.-R. Song, H.-Q. Fu, C.-Y. Yue and X.-W. Lei, Ultrastable 0D Organic Zinc Halides with Highly Efficient Blue Light Emissions, *Adv. Opt. Mater.*, 2022, **10**, 2200386.

54 J.-Q. Zhao, H. Ge, Y.-F. Wu, W.-J. Xu, K. Xu, J.-Q. Ma, Q.-L. Yang, C.-Y. Yue and X.-W. Lei, Crystal rigidifying strategy toward hybrid cadmium halide to achieve highly efficient and narrowband blue light emission, *Mater. Today Chem.*, 2022, **24**, 100766.

55 Y. Li, C. Ji, L. Li, S. Wang, S. Han, Y. Peng, S. Zhang and J. Luo, $(\gamma$-Methoxy propyl amine$)_2PbBr_4$: a novel two-dimensional halide hybrid perovskite with efficient bluish white-light emission, *Inorg. Chem. Front.*, 2021, **8**, 2119–2124.

56 D.-Y. Li, Y.-H. Liu, Q. Wang, X.-W. Lei, C.-Y. Yue and Z.-H. Jing, Zero-dimensional hybrid zinc halides with blue light emissions, *Mater. Today Chem.*, 2023, **31**, 101604.

 This journal is © the Partner Organisations 2024